AJNR

Clinical proton MR spectroscopy of neurodegenerative disease in childhood.

A A Tzika, W S Ball, Jr, D B Vigneron, R S Dunn and D R Kirks

AJNR Am J Neuroradiol 1993, 14 (6) 1267-1281
http://www.ajnr.org/content/14/6/1267

Clinical Proton MR Spectroscopy of Neurodegenerative Disease in Childhood

A. Aria Tzika,[1-4] William S. Ball, Jr,[1,2] Daniel B. Vigneron,[3] R. Scott Dunn,[1] and Donald R. Kirks[1,2,4]

PURPOSE: To determine the contribution of MR spectroscopy in the assessment of childhood neurodegenerative disease. **METHODS:** Fifty-one subjects (7 weeks to 17 years of age), 22 with either hereditary (n = 16) or acquired (n = 6) neurodegenerative disorders and 29 age-matched control subjects, were studied with combined proton MR spectroscopy and MR imaging. Single-voxel (2.0–8.0 cc) MR spectra were acquired at 1.5 T, with either short-echo–stimulated echoes and/or long-echo spin echoes. **RESULTS:** MR spectra exhibited signals from n-acetyl-, creatine-, and choline-containing compounds, neurotransmitters (glutamate), intracellular mediators (inositols), and glycolytic products (lactate). Abnormal MR spectra in neurodegenerative disorders reflected: demyelination, neuronal loss, and gliosis (increased mobile lipid presence and reduction of n-acetylaspartate to choline); metabolic acidosis (lactate accumulation); and neurotransmitter neurotoxicity (increased glutamate, glutamine, and inositols). **CONCLUSION:** Proton MR spectroscopy may complement MR imaging in diagnostic assessment and therapeutic monitoring of neurodegenerative disorders.

Index terms: Degenerative brain disease; Children, central nervous system; Brain, magnetic resonance; Magnetic resonance, spectroscopy; Pediatric neuroradiology

AJNR 14:1267–1281, Nov/Dec 1993

Neurodegeneration occurs in a number of devastating disorders of childhood, which can be either hereditary and/or acquired (1). Neuropathologic findings may show either primary gray- and/or white-matter involvement or no recognizable gross abnormality (2). Clinical findings are usually nonspecific, and laboratory tests are of limited value. Imaging modalities demonstrate the results of abnormal cellular function on organ morphology. Both computed tomography and magnetic resonance (MR), with MR being more sensitive, may demonstrate degenerative changes in the central nervous system (3). However, the specificity of MR is limited and is dependent on optimization of MR image quality and interpretation (4). MR assessment of neurodegeneration is especially difficult in children, in whom white-matter signal intensity changes during normal brain development with progressive myelination (5).

To enhance the specificity of MR in the assessment of neurodegenerative disease, proton MR spectroscopy (MRS) may provide additional insight into in vivo metabolism. MR shows gross structural changes that are presumably caused by underlying metabolic abnormality. Proton MRS can noninvasively detect metabolite levels and thus may allow an earlier and more specific determination of neurodegeneration. Furthermore, the capability of performing serial examinations by image-guided proton MRS may aid in monitoring the success or failure of new treatment regimens. Proton MRS studies have been used infrequently because of water suppression and spatial-localization requirements. Recent hardware and software advances have permitted

Received July 23, 1992; accepted pending revision September 13; revision received November 18.

Presented in part at the 35th Annual Meeting of The Society for Pediatric Radiology, Orlando, Fla, May 1992.

[1] Department of Radiology, Children's Hospital Medical Center, Cincinnati, OH 45229.

[2] Departments of Radiology and Pediatrics, University of Cincinnati College of Medicine, Cincinnati, OH 45229.

[3] Magnetic Resonance Science Center, University of California San Francisco, San Francisco, CA 94143.

[4] Current Address: Departments of Radiology, Children's Hospital and Harvard Medical School, Boston, MA 02115.

Address reprint requests to A. Aria Tzika, PhD, Department of Radiology, Children's Hospital, 300 Longwood Ave, Boston, MA 02115.

AJNR 14:1267–1281, Nov/Dec 1993 0195-6108/93/1406–1267

preliminary evaluation of neurodegenerative changes and demyelination in adult humans with multiple sclerosis (6, 7). A recent report on a study of children (8) describes in vivo MRS findings with destructive brain disease but uses only long-echo spectra. We have used a combined protocol of short and long echoes to increase the number of MR-visible metabolites. In addition, we have applied optimized radio-frequency pulses to improve localization, increase water suppression, and allow smaller voxels of interest, while maintaining a good signal-to-noise ratio.

The purpose of this study was to determine whether proton MRS contributes additional information to the assessment of neurodegenerative disorders of childhood. The underlying hypothesis was that proton MRS, known to provide insight into metabolism in vivo, would detect changes in patterns of metabolites; these should indicate certain aspects of the neurodegenerative process.

Methods

Subjects

Fifty-one subjects, ranging in age from 7 weeks to 17 years, participated in the study. Informed consent was obtained from the parents of all subjects. All studies were performed with approval of the Committee on Clinical Investigations.

Table 1 shows the four separate age groups of 29 control children, including healthy volunteers (n = 16) and patients studied for reasons other than neurodegenerative disease (n = 13). Criteria for inclusion of control subjects were normal MR findings and absence of any clinical history or physical findings of neuropathy. Table 2 lists 22 children with various types of neurodegenerative disorders. Criteria for inclusion in this group were a positive clinical history and abnormal neurologic examination and/or laboratory findings.

In children younger than 2 years of age, sedation consisted of either oral chloral hydrate (100 mg/kg) or intravenous pentobarbital (Nembutal; Abbott Laboratories, North Chicago, Ill; 3–6 mg/kg). All sedated patients were monitored by electrocardiography and pulse oximetry.

TABLE 1: Grouping of control children

Age Group (Age Interval)	No. of Children
Neonate, infant (2–23 months)	5
Early childhood (2–4 years)	4
Late childhood (9–13 years)	17
Adolescence (14–17 years)	3

TABLE 2: Grouping of children with neurodegenerative brain disorders (age range: 4 months to 16 years)[a]

Disorder	No. of Children
Hereditary	(16)
Peroxisomal disorder	5
Lysosomal storage disease	3
Mitochondrial dysfunction	1
Disorders of amino acid and organic acid metabolism	1
White matter disorder with unknown metabolic defect	3
Neurofibromatosis	3
Acquired	(6)
Hypoxia-ischemia	4
Toxic encephalopathy	2

[a] According to classification of Valk and van der Knaap (1).

MR Image-Guided Proton MR Spectroscopy

MR image-guided proton MRS was performed in conjunction with the clinical MR protocol on a 1.5-T whole-body MR system (General Electric Medical Systems, Milwaukee, Wis) using a quadrature head coil. Intravenous gadopentetate dimeglumine (Magnevist; Berlex Laboratories, Wayne, NJ; 0.1 mmol/kg) was administered in some cases, after spectroscopy, to detect blood-brain-barrier abnormalities.

MR images were obtained using a clinical MR protocol that includes spin-echo T1-weighted images (500/12/2 [repetition time/echo time/excitations]) and T2-weighted images (2500/30 and 100). Sagittal and axial MR images were acquired using the spin-echo sequences (256 × 192 matrix, 5-mm thickness, 1-mm gap). Fast spin-echo imaging (2500/19 and 120) was performed on certain occasions, when dictated by time constraints. The imaging protocol was completed within 25 to 40 minutes depending on the use of fast spin-echo or conventional spin-echo sequences.

MR images were used to guide the volume-of-interest selection for single-voxel MRS. The selection of voxel size and position was determined visually by examining the voxel images in all three dimensions. Localized field homogeneity (shimming) was optimized using linear- and, where necessary, higher-order shim coils with either a stimulated echo-acquisition mode (STEAM) and/or point-resolved spectroscopy (PRESS). The typical shim value range was 0.06 to 0.14 ppm over the volume of interest. Acquisition parameters for STEAM were 2000/18, mixing time 10.8 msec, 256 acquisitions, 2000 complex data points, and 2 kHz receiver band width. Acquisition parameters for PRESS were the same as for STEAM except echo time was 135 or 270 msec. Voxel dimensions ranged from 2.0 to 8.0 cc.

All spectra were processed on a remote SUN 3/470 work station (SUN Microsystems, Mountain View, Calif) using the Spectroscopy Analysis software by General Electric. Exponential multiplication of 1.5 Hz and Fourier transformation were followed by phase correction. No other mathematical manipulations such as resolution enhancement, baseline correction, or other fitting routines were

applied. Spectral assignments were performed as previously described (9, 10), with n-acetylaspartate (NAA) set to 2.01 ppm.

Descriptions of the localization procedures of STEAM and PRESS have been previously reported (11, 12). Improved versions of these procedures were recently implemented on a General Electric Signa 1.5-T system. These versions make use of optimal frequency–selective excitation radio-frequency pulses (13). For both methods, three of these pulses provide three-dimensional spatial localization in the presence of mutually orthogonal field gradients in a single acquisition. For short-echo (18 msec echo time) acquisitions, STEAM was the method of choice, because such an echo time could not be achieved with PRESS (14). Short echo permits identification of short-T2 and/or strongly coupled metabolites and increases the number of metabolites detectable by in vivo proton MRS (9, 15, 16). Nevertheless, a major disadvantage of using STEAM is the twofold loss in signal inherent to the stimulated echoes (17). To detect lactate without the overwhelming presence of lipids at the same chemical shift, long-echo acquisitions were required (18). The lactate spectrum is composed of a doublet because of its $-CH_3$ protons at 1.33 ppm and a quartet because of its $-CH$ protons at 4.3 ppm (close in proximity to the water that was observed in vivo). These are coupled with a coupling constant (J) of 7.35 Hz. At an echo time 270 (2/J), the methyl resonances of lactate are completely refocused. In addition, the amplitude of the 1.33-ppm lactate doublet is increased approximately twofold when PRESS is used instead of STEAM. For long-echo acquisitions, we use PRESS with an echo time of 270 to enhance our sensitivity for lactate detection (19).

Water suppression was achieved using a repetition of chemical-shift-selective radio-frequency pulses followed by dephasing-gradient pulses (20). The chemical-shift-selective sequences are designed to avoid occurrence of unwanted echoes and interference with the localization scheme.

Results

Control Children

Good-quality localized water-suppressed proton MR spectra were acquired. The quality of localization is demonstrated by the sharp margins of the images representing the voxels of interest (Fig 1B). Effective water suppression of up to approximately 10 000-fold is indicated by the reduced presence of water in the proton MR spectra of Figures 1C and 1D. As illustrated in Figures 1 and 2, the spectra from control subjects demonstrated prominent metabolite peaks because of the protons of the methyl (CH_3) group of NAA at 2.01 ppm (found primarily in neurons, thus implicated as a neuronal marker), creatine compounds (creatine [Cr] and phosphocreatine [PCr]) at 3.03 and 3.94 ppm (intracellular compounds involved in cellular energetics), and choline (Cho)-containing compounds such as phosphocholine and glycerophosphocholine at 3.22 ppm (membrane constituents). In addition, short-echo STEAM spectra revealed the presence of broad peaks because of the protons of short-chain fatty acids and mobile protein moieties (lipids) at 0.9 and 1.2 ppm (21–24). Furthermore, short-T2 and/or strongly coupled metabolites were detected. These included glutamate (excitatory neurotransmitter), glutamine (Glx; involved in glutamate biosynthesis) at two separate locations of the spectra 2.0 to 2.55 ppm and 3.65 to 3.85 ppm, and inositol compounds (Inls) at 3.56 to 3.77 ppm (intracellular mediators). Additional compounds such as γ-aminobutyric acid (2.25 ppm), glycine (3.5 ppm), taurine (3.3 ppm), and aspartate (2.8 ppm), all of which are amino-acid neurotransmitters, may be detected (9).

Table 1 divides the 29 control children into four separate groups according to age. These age groups were used in the comparative interpretation of spectra from children with neurodegenerative diseases. Age-matched comparisons are critical because proton-brain MR spectra reflect metabolic changes occurring during the course of early brain development (25–28). The difference in the relative prominence of the metabolite peaks during early brain development is demonstrated by comparison of the spectra in Figure 2 from a 7-week-old healthy neonate to the spectra from a 2-year-old healthy child (Fig 1). The most striking changes at 2 years of age include increased relative presence of NAA, and decrease of Inls (10). Indeed NAA becomes the most pronounced peak in the proton spectra of the brain by approximately 6 months of age, whereas Inls become less prominent by 18 months of age. The ratio of Cho-containing compounds to creatines increases with brain development, as evidenced by the relative peak intensities of these compounds in the PRESS spectra of Figures 1 and 2. By early childhood (2–4 years) the increase in NAA is nearly completed, and by late childhood (9–13 years) the NAA signal is twice that of Cho. In addition, Cho increases relative to creatines with increasing age.

Children with Neurodegenerative Disorders

Hereditary Neurodegenerative Disorders

Peroxisomal Disorders. Five boys with X-linked adrenoleukodystrophy were studied. Three children (7–9 years old) with neurologic manifes-

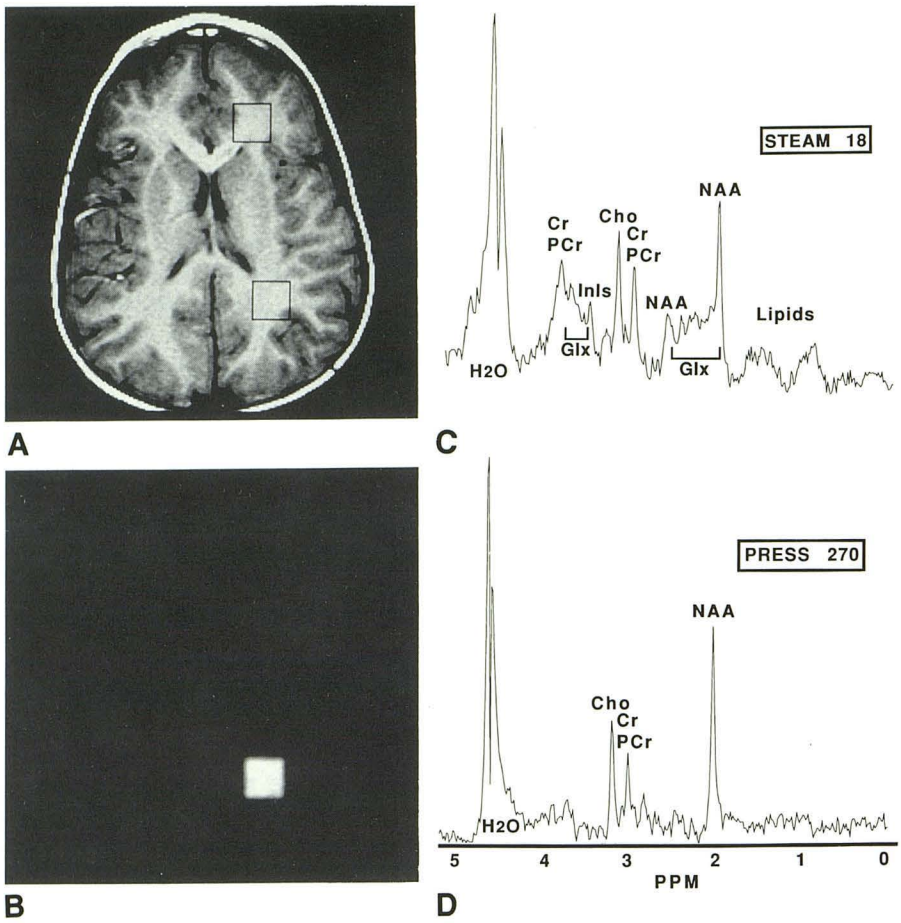

Fig. 1. Image-guided single-voxel proton MRS using a 3.4-cc voxel (*square*) of interest chosen from axial brain MR images of a 2-year-old healthy boy.

A, T1-weighted image (500/12). The myelination pattern and the gray-to-white matter contrast are normal for 2 years of age.

B, Occipital white-matter-voxel MR image (400/18) using STEAM. The quality of the spectroscopy localization scheme used is demonstrated by the sharp edges of the MR image of the voxel.

C and *D,* Localized proton MR spectra from the voxel indicated in *A*. Limited presence of water in both spectra demonstrates effective water suppression. *C,* Short-echo proton MR spectrum (2000/18) using STEAM. Most noticeable peaks are NAA, Cr and PCr compounds, Cho-containing compounds, and Inls. Additional discernible resonances are: the 2.6-ppm resonance of NAA; the Glx area from 2.0 to 2.55 ppm containing glutamate, Glx, and γ-aminobutyric acid; the Glx area from 3.65 to 3.85 ppm containing glutamate, Glx, and glucose; Inls compounds at 3.56 to 3.77 ppm; glycine at 3.55 ppm; and the 0.8- to 1.2-ppm broad resonances containing mobile moieties of cytosolic proteins and short-chain fatty acids (lipids). *D,* Long-echo proton MR spectrum using PRESS (2000/270). Prominent peaks are NAA, Cho, and Cr/PCr. Inls, Glx, and lipid peaks are reduced or absent.

tations of the disease revealed abnormal MR and proton MRS findings, which were similar in all three cases. Figure 3 includes MR images and proton MR spectra of one representative case. Abnormal bright signal was found in the posterior parietal and occipital white matter on T2-weighted (Fig 3A) and proton-density (Fig 3B) MR images. Proton MR spectra, from a voxel of interest localized within the area of bright signal, exhibited a virtual absence of NAA, increased presence of Inls and/or glycine, and a lactate peak (Fig 3C). Lactate was also detected in the long-echo PRESS spectra (Fig 3D), where lipid signals are minimal. The peak at 3.55 ppm in these spectra is presumably caused by the $-CH_2$ protons of glycine, with a relatively long T2 (9). Two additional children (2 and 17 years of age), while carrying the X-linked defect for adrenoleukodystrophy and normal neurologic findings, exhibited MR and proton MRS similar to age-matched healthy volunteers.

Lysosomal Storage Disease. Three patients were studied: one with Sanfilippo syndrome (mucopolysaccharidosis type IIIA) (a 2-year-old girl), one with Gaucher disease (a 6-month-old boy), and one with Hurler syndrome (a 5-year-old boy). All three cases exhibited a delay in myelination as evidenced by MR. In addition, the contrast of

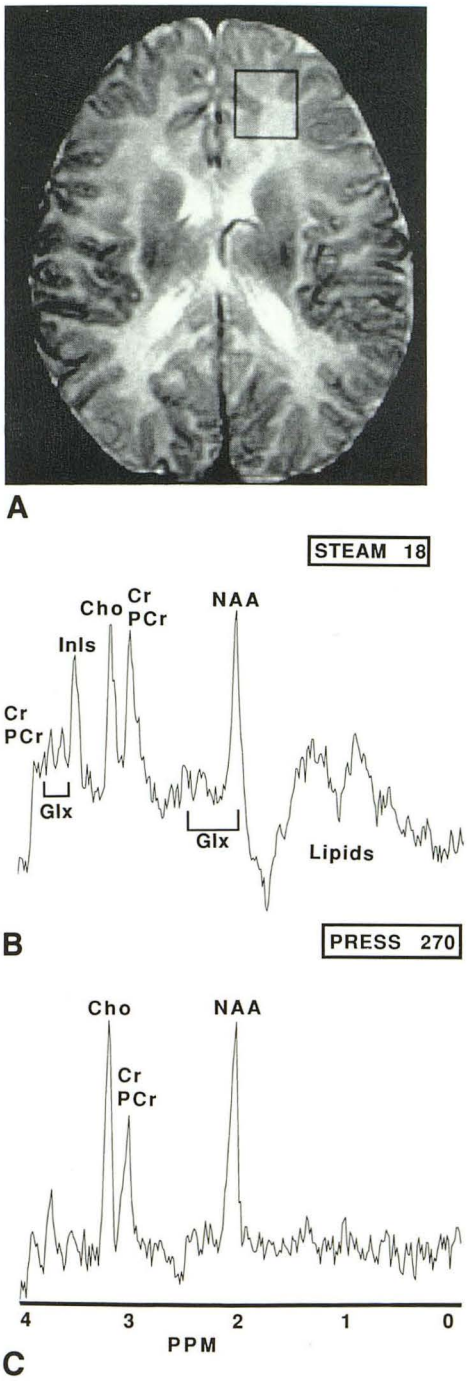

Fig. 2. Image-guided single-voxel proton MRS using a 3.7-cc voxel (*square*) of interest chosen from axial brain MR images of a 7-week-old healthy boy.

A, T2-weighted image (3000/100). The myelination pattern and the reversed gray-to-white matter contrast are normal for 7 weeks of age.

B and *C*, Localized proton MR spectra from the voxel indicated in *A*. *B*, Short-echo proton MR spectrum using STEAM (2000/18). *C*, Long-echo proton MR spectrum using PRESS (2000/270). Note that the intensity of NAA relative to Cho is lower, and Inls are relatively higher, as compared with older age (Fig 1).

gray matter to white matter on proton-density and T2-weighted images was altered because of increased signal within the white matter. Figure 4 shows MR images and spectra from the Sanfilippo case. By comparison with the images from an age-matched healthy child (Fig 1), the difference in the gray-to-white matter contrast can be qualitatively assessed. Proton spectra exhibited a reduced NAA-to-Cho ratio for age (Figs 4C and 4D); short-echo STEAM (Fig 4C) revealed an enhanced presence of Glx and/or Inl resonances and elevated lipid resonances. Figure 5 contains representative images and a short-echo STEAM spectrum from a 6-month-old neonate with Gaucher disease. MR images were normal for age (Figs 5A and 5B). In contrast to Figure 4C, MR spectra exhibited a normal intensity NAA for this age. The presence of Inls, however, was elevated. The Hurler case revealed both decreased NAA-to-Cho detection and increased Glx and Inls in a posteriorly located white-matter short-echo STEAM spectrum.

Mitochondrial Dysfunction. Figure 6 illustrates characteristic MR images and proton spectra of a 4-month-old boy with Leigh disease. Laboratory findings indicated metabolic acidosis. MR images showed decreased signal intensity in selected brain regions, especially the basal ganglia (Fig 6A). The same regions exhibited pronounced bright signal in T2-weighted images (Fig 6B). Proton spectra from a voxel of interest placed in the region of the lentiform nucleus exhibited an extremely high level of lactic acid (Figs 6C and 6D), which is normally undetectable in proton MR spectra of healthy children. Because of the low signal-to-noise ratio, assessment of other metabolites in the short-echo STEAM spectrum was not possible (Fig 6C); however, the long-echo PRESS spectrum revealed normal presence of NAA, Cho, and creatines for age (Fig. 6D). In this spectrum, the ratio of observed lactate to NAA was 5.50.

Disorders in Amino Acid and Organic Acid Metabolism. In an 18-month-old boy with phosphorylase kinase deficiency and hepatosplenomegaly, levels of serum lactate and pyruvate were three times that of normal (atypical glycogen storage disease type IX). Short-echo STEAM spectra of parietooccipital white matter and MR images were normal.

Unknown Metabolic Defect in White-Matter Disorder. Figure 7 shows the results from image-guided proton MRS in a 12-month-old boy with a white-matter abnormality of undetermined ori-

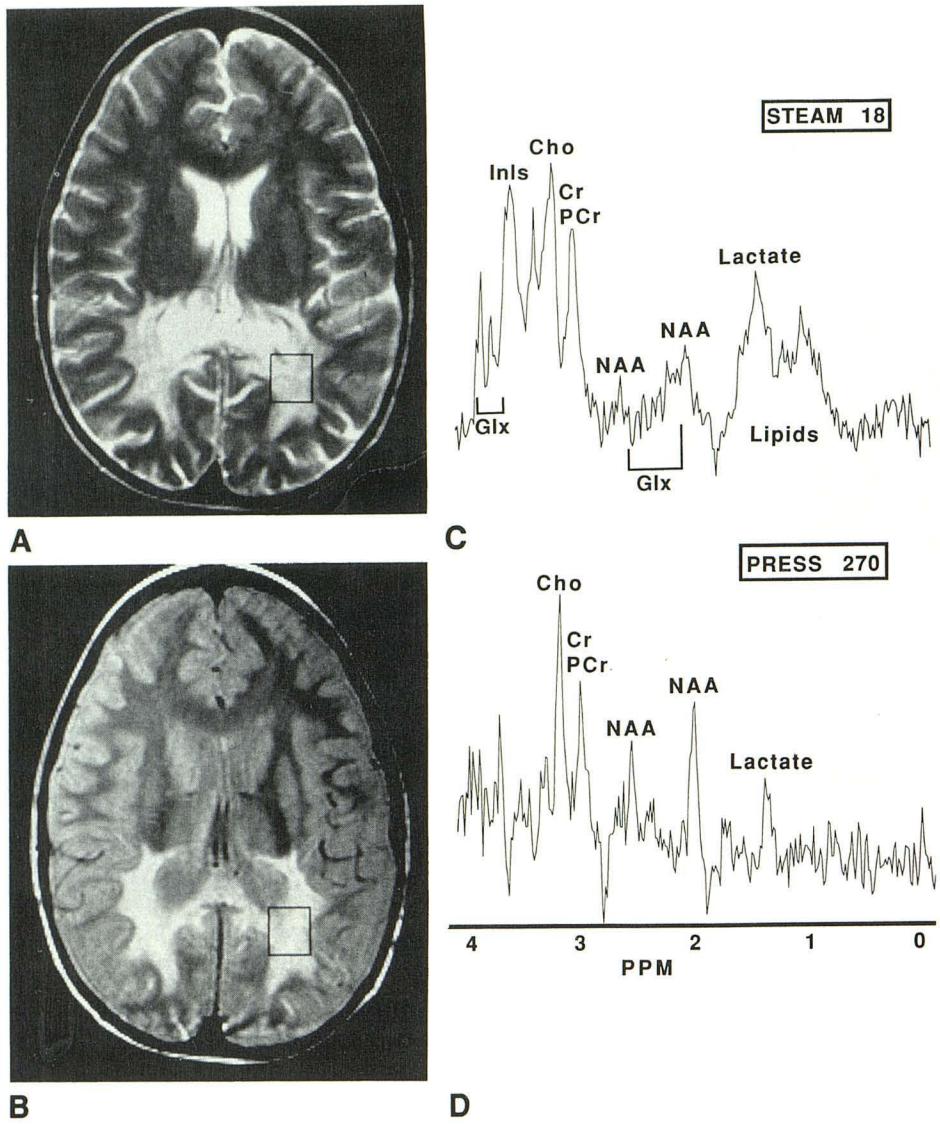

Fig. 3. Image-guided single-voxel proton MRS using a 3.4-cc voxel (*square*) of interest chosen from axial brain MR images of a 8-year-old boy with adrenoleukodystrophy.

A, T2-weighted (2500/120) fast spin-echo MR image shows bilateral occipital white matter lesions typical of adrenoleukodystrophy.

B, Proton density (2500/19) fast spin-echo MR image. Better separation of ventricles and white matter permits selection of the voxel of interest within the hyperintense abnormal occipital white matter.

C, Short-echo proton MR spectrum of an occipital voxel of interest, selected from image *B*, using STEAM (2000/18). Substantial reduction of NAA relative to Chos (Cho) and spared creatines (Cr, PCr) may indicate neurodegeneration and gliosis. Enhanced Inls (Inls) and lipids may be associated with encephalopathy and demyelination, respectively.

D, Long-echo proton MR spectrum using PRESS (2000/270). Relative presence of NAA to Chos is observed in addition to a peak at 1.33 ppm presumed to be lactic acid.

gin, possibly caused by an unrecognized metabolic defect. T2-weighted MR images exhibited abnormally high signal in the white matter (Fig 7A) compared with healthy age-matched children. No specific pattern in this bright signal was observed, and the white matter appeared brighter compared with the gray matter for age. The proton MR spectra showed reduced NAA-to-Cho presence for age and an enhanced lipid presence in the short-echo STEAM (Fig 7B and 7C).

Figure 8 shows images and proton MR spectra from a 3-year-old girl with a possible metachromatic leukodystrophy. MR findings include focal bright signal in the frontoparietal white-matter region (Fig 8A) in an otherwise normal brain. Proton MRS revealed enhanced lipids and Glx in

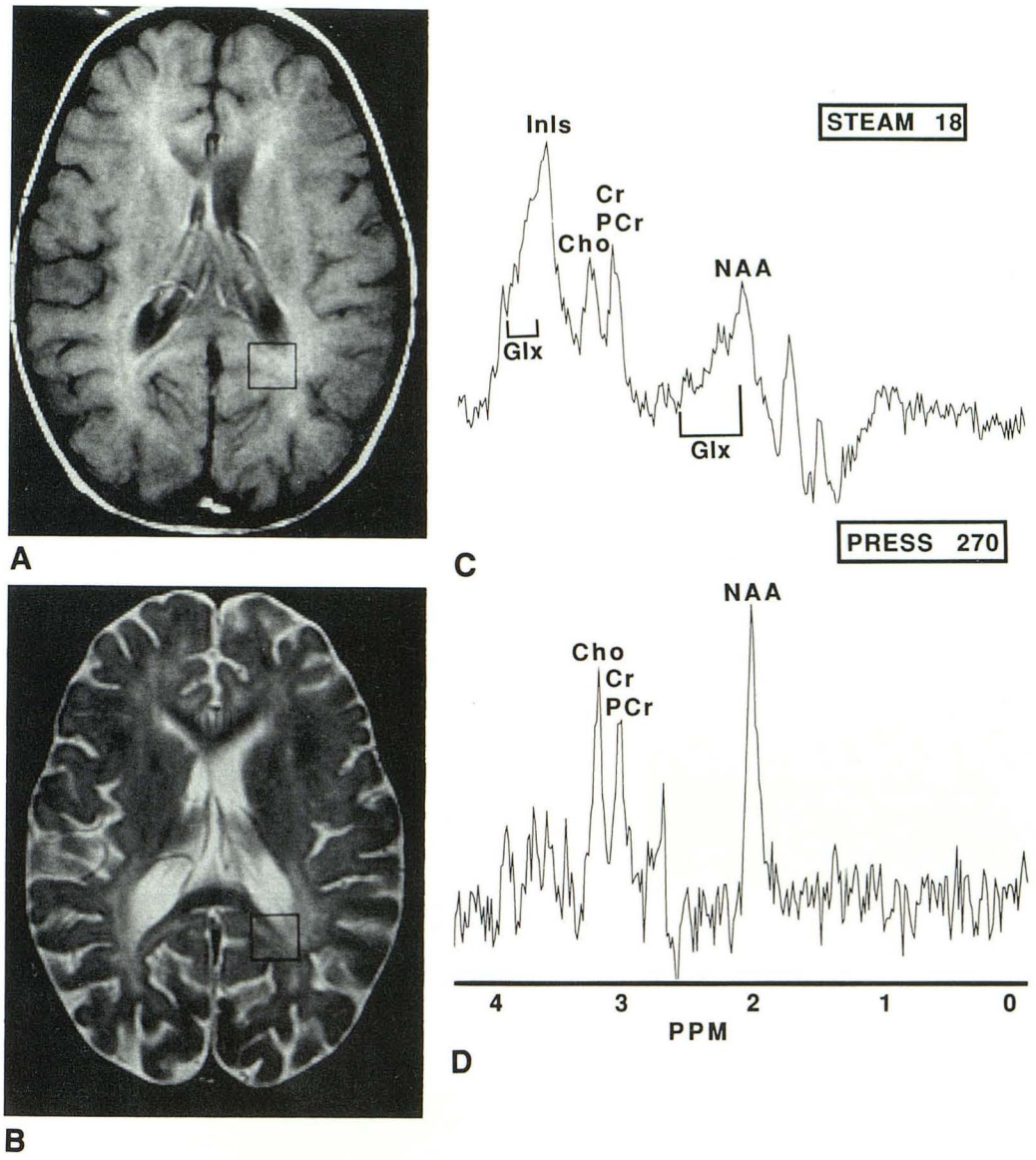

Fig. 4. Image-guided single-voxel proton MRS using a 3.2-cc voxel (*square*) of interest chosen from axial brain MR images of a 2-year-old girl with Sanfilippo (mucopolysaccaridosis type IIIA) syndrome.

A, Proton-density image (2500/30).

B, T2-weighted image (2500/100). Note the altered gray-to-white matter contrast compared with the images of an age-matched subject. This alteration is related to depositions of glycosaminoglycans in subendothelial locations of the central nervous system known to occur in this disease.

C and *D*, Localized proton MR spectra from the voxels indicated in *A* and *B*. *C*, Short-echo proton MR spectrum of occipital white matter using STEAM (2000/18). *D*, Long-echo proton MR spectrum using PRESS (2000/270). Note the reduced presence of NAA relative to Cho in both spectra. In addition, enhanced presence of glutamate, Glx, glycine, and/or Inls compounds and elevated lipid resonances may represent encephalopathy and gliosis.

the short-echo STEAM spectrum (Fig 8B) and an essentially normal PRESS (Fig 8C) compared with the healthy 2-year-old child in Figure 1.

In yet another case, where white-matter lesions were detected by MR in a 6-month-old boy, reduced NAA-to-Cho and elevated Glx and Inls were observed in the spectra.

Neurofibromatosis. In children with neurofibromatosis (7–9 years of age), lower NAA and higher Glx and Inls were detected in one child, compared with control subjects of the same age; another child (7 years old) presented normal MR and proton MR spectra of the white matter; and another child (9 years old) had abnormal signal in

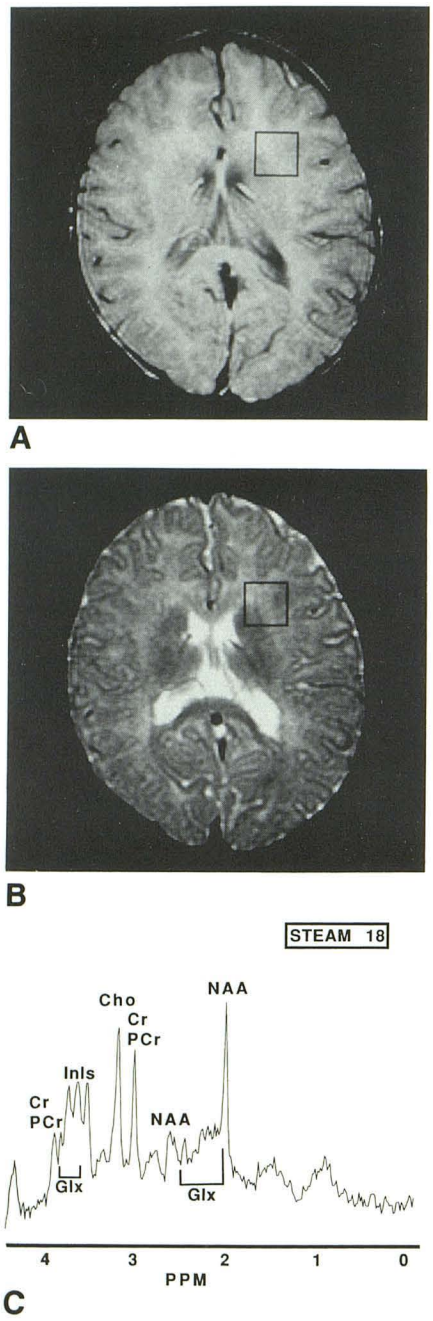

Fig. 5. Image-guided single-voxel proton MRS using a 3.2-cc voxel (*square*) of interest chosen from axial brain MR images of a 6-month-old boy with Gaucher disease.

A, Proton-density image (2500/30).

B, T2-weighted image (2500/100).

C, Short-echo proton MR spectrum of a voxel of interest located within the white matter using STEAM (2000/18). The spectrum exhibits multiple peaks at 3.55 to 3.9 ppm (Glx/Inls). No relative reduction of NAA is observed.

the globus pallidus in addition to multiple patchy areas of increased signal in the medulla, pons, and middle cerebellar peduncles on the T2-weighted MR images. Proton MR spectra localized to signal abnormalities in the deep gray matter showed lower NAA and increased Glx.

Acquired Neurodegenerative Disorders

Hypoxia-Ischemia. Figure 9 displays the MR images and spectra from a 9-year-old boy with subacute stroke. Blood-brain-barrier breakdown with enhancement is shown in the postcontrast T1-weighted MR image (Fig 9A). Edema is depicted in the T2-weighted images (Fig 9B), and abnormal bright signal is detected in the adjacent occipital white-matter region. Proton MR spectra of a voxel of interest located in this region showed a reduced NAA-to-Cho ratio for a 9-year-old child and increased Glx and/or Inls (Fig 9C). A lactic acid peak is clearly evident in the long-echo PRESS spectrum (Fig 9D), because the presence of lipids is minimal in comparison with the short-echo STEAM spectrum (Fig 9C). In all three additional cases of suspected stroke (ages 4 months to 11 years), the NAA-to-Cho ratio was reduced, and in one case Glx was clearly elevated in the region of infarction.

Toxic Encephalopathy. Two children with gestational exposure to cocaine were examined (18 months and 3 years). In both cases, no gross abnormalities were detected by either MR imaging or MRS.

Discussion

Neurodegenerative disorders can affect gray and/or white matter of the brain and have been classified either according to the presence or absence of a specific metabolic defect or according to their effect on myelination (demyelinating versus dysmyelinating disorders). Our material has been categorized according to the classification proposed by Valk and Van der Knaap in 1989 (1). A similar classification can be used for categorizing neurodegenerative diseases in general. One should include one additional factor in this categorization, the static or chronic mode of the disease (29). This is, however, beyond the scope of the current study, as we have not yet performed examinations over an extended period of time on such patients. Our discussion is thus limited to one-time observations for a variety of disorders affecting the brain in children.

Hereditary Neurodegenerative Disorders

Peroxisomal Disorders. These disorders have been associated with defects in the peroxisome structure and/or defects of single or multiple

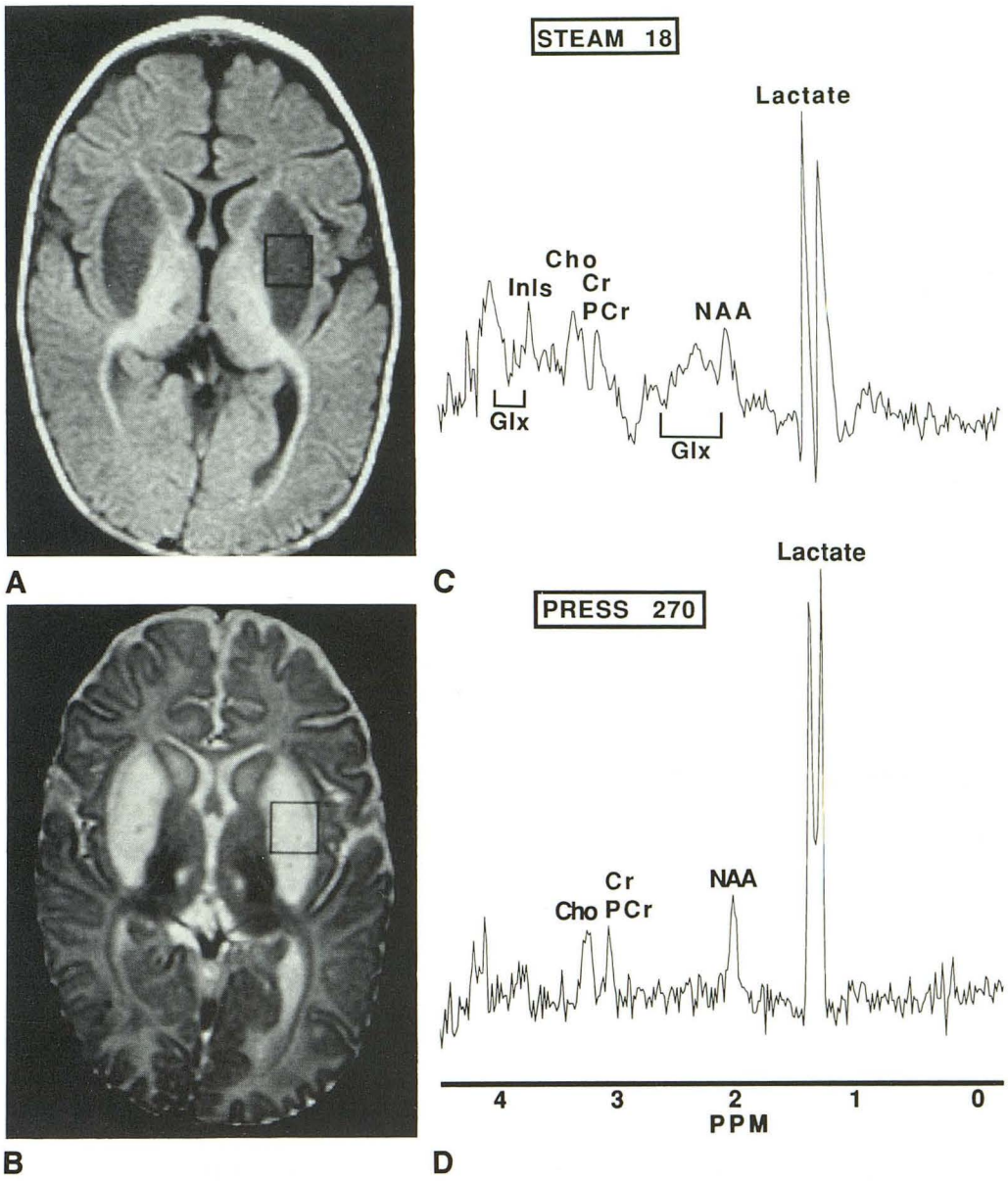

Fig. 6. Image-guided single-voxel proton MRS using a 3.4-cc voxel (square) of interest chosen from axial brain MR images of a 4-month-old boy with Leigh disease.

A, Inversion recovery T1-weighted image (2000/800) shows hypointense lentiform nuclei bilaterally.

B, T2-weighted image (2500/100) with characteristic pattern of bilateral bright lentiform nuclei. The myelination pattern and the reversed gray-to-white matter contrast are compatible with 7 weeks of age.

C and *D,* Localized proton MR spectra from the voxel indicated in *A* and *B. C,* Short-echo proton MR spectrum using STEAM (2000/18). Increased lactic acid is detected. Other metabolites are not clearly resolved because of signal-to-noise considerations. *D,* Long-echo proton MR spectrum using PRESS (2000/270). Note an extremely large amplitude of lactate signal compared with the other resonances.

peroxisomal enzymes. The defect is transmitted by an autosomal-recessive or an X-linked mode of inheritance. The classification of peroxisomal disorders, as proposed, includes three separate groups (30): group 1, in which peroxisomes are absent or reduced and activities of multiple peroxisomal enzymes are deficient (Zellweger cerebrohepatorenal syndrome, neonatal adrenoleukodystrophy, hyperpipecolic acidemia, and infantile Refsum disease); group 2, in which the number of peroxisomes is normal and only a single peroxisomal enzyme is reduced (X-linked adrenoleukodystrophy, acatalasemia, pseudo-Zellweger syndrome, acetyl-coenzyme A oxidase deficiency, and bifunctional enzyme deficiency); and group 3, in which structurally abnormal peroxisomes and multiple enzymatic defects occur (rhizomelic chondrodysplasia punctata).

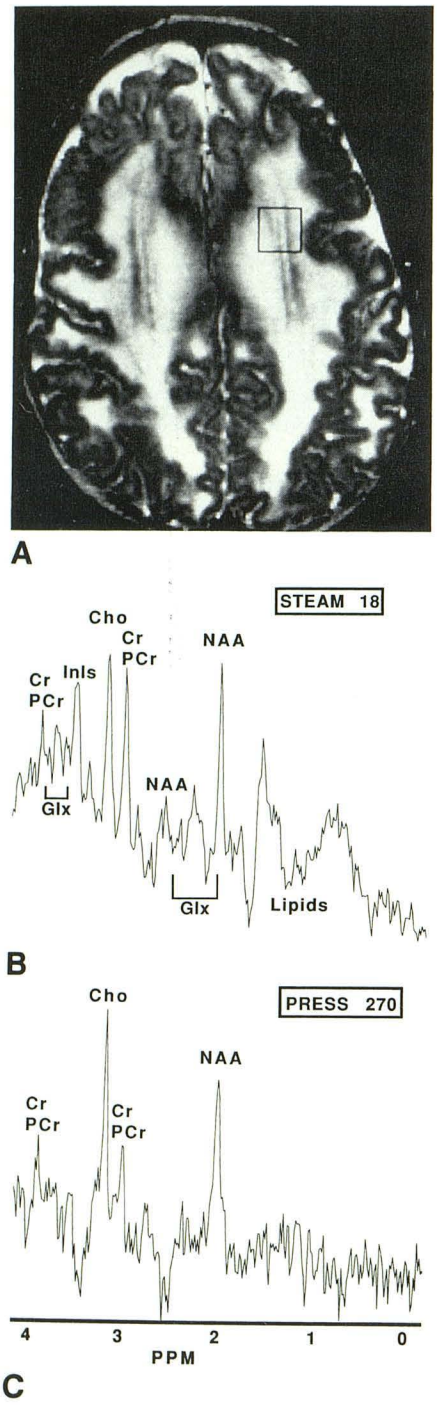

Fig. 7. Image-guided single-voxel proton MRS using a 3.4-cc voxel (*square*) of interest chosen from axial brain MR images of a 12-month-old boy with an unknown metabolic disease affecting cerebral white matter.

A, T2-weighted image (2500/100) of a 12-month-old boy with an unknown metabolic disease affecting cerebral white matter. Note abnormal white matter signal.

B and *C*, Localized proton MR spectra from the voxel indicated in *A*. *B*, Short-echo proton MR spectrum using STEAM (2000/18). Enhanced lipid presence indicates demyelination. *C*, Long-echo proton MR spectrum using PRESS (2000/270). Note that the relative height of NAA peak to Cho is reduced for this age.

Noninvasive diagnostic laboratory assays currently available include assessment of long-chain fatty acids in plasma, cultured skin fibroblasts, and chorionic villi, as well as measurement of pipecolic acid, bile acid intermediates, and phytanic acid oxidase levels (31). In addition, imaging modalities such as computed tomography and MR can define characteristic patterns, with MR being more sensitive than computed tomography (32, 33).

Our observations are primarily of the most common peroxisomal disorder, X-linked adrenoleukodystrophy, which is associated with lignoceroyl-coenzyme A ligase deficiency (34). This enzymatic defect prevents the breakdown of very long-chain fatty acids, leading to their accumulation primarily in adrenal cortex and cerebral white matter. Incorporation of very long-chain fatty acids in myelin renders the myelin unstable (35). Neurologic symptoms begin in affected boys between 5 and 7 years of age and may be preceded by adrenal insufficiency. Behavioral disorders and progressive neurologic deterioration eventually lead to a vegetative state and death (36). The symmetrical alteration of white matter is usually first imaged in posterior brain and is consistent with our observations in three affected boys (representative case illustrated in Fig 3). These alterations in MR signal intensity of the white matter are accompanied by striking changes in proton MR spectra and include absence of NAA, implicated to be a neuronal marker (37, 38), preserved creatines and enhanced Chos, indicative of neurodegeneration and gliosis. Increased resonances in the Glx areas of the short-echo STEAM spectra indicate increased excitatory neurotransmitter concentration and may suggest neurotransmitter imbalances associated with the neurodegeneration process (39). Inls compounds also may be increased; however, their increased presence cannot always be resolved from changes in glycine (another excitatory amino acid detected at the same chemical shift with Inls at 3.5 ppm). Inls compounds are intracellular messengers, and their increase may be associated with excitatory-amino-acid neurotoxicity (40, 41). When these compounds increase above 1 mM and are visible on the MR spectra, this also may indicate neurodegeneration. The limited presence of lactic acid in the long-echo spectra in adrenoleukodystrophy is probably nonspecific and can be attributed to reduced local blood perfusion. This leads to accumulation of lactic acid, which is not effectively

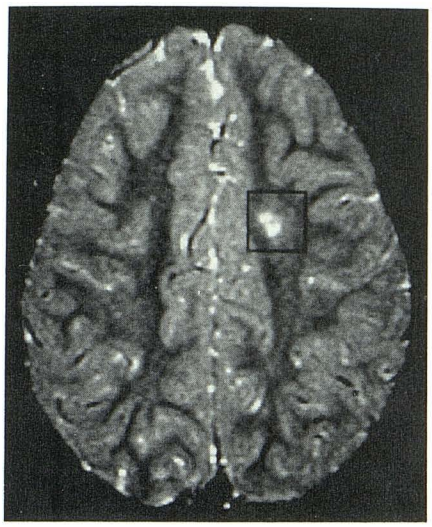

A

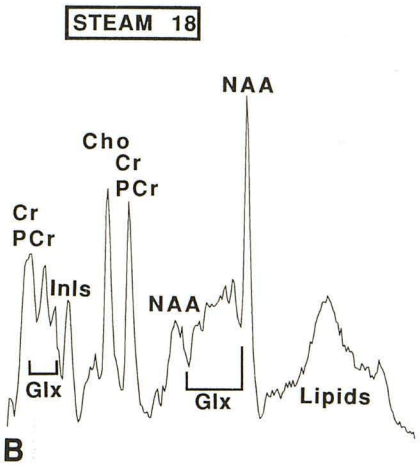

B

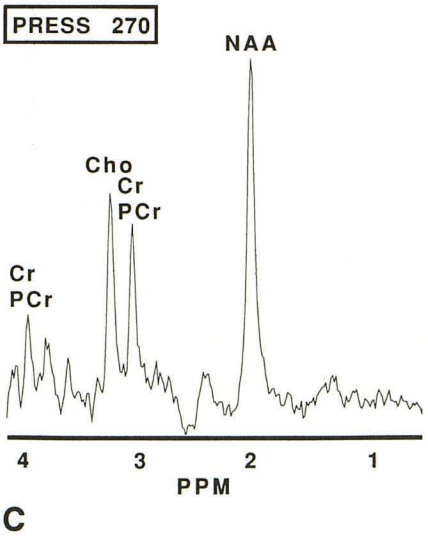

C

Fig. 8. Image-guided single-voxel proton MRS using a 7.6-cc voxel (*square*) of interest chosen from axial brain MR images of a 3-year-old girl with white matter disease from an unknown metabolic defect.

A, T2-weighted image (2500/100). Note the left-frontoparietal white-matter lesion.

removed by the blood circulation. If proton MR can detect these types of changes in vivo, it may become an important tool in the evaluation of neurodegenerative changes in peroxisomal disorders. This hypothesis, supported by our observations, must be tested in animal models of disease as well as in larger numbers of patients.

Lysosomal Storage Disease. These disorders are caused by lysosomal enzyme defects, which are inherited in an autosomal-recessive manner. The nervous system is affected either directly, because of intraneuronal accumulation of materials not degraded by lysosomes, or indirectly, because of meningeal and axial-skeletal involvement (42, 43). The disorders are classified according to the accumulated material in the lysosomes: mucopolysaccharidosis (Sanfilippo and Hurler syndromes), lipidoses (Gaucher disease, gangliosidosis G_{M1} and G_{M2}, and Nieman-Picksyndrome), and mucolipidoses.

In our three cases of lysosomal storage disease, proton MRS of white matter indicated neurodegenerative changes despite the absence of MR findings. In Sanfilippo syndrome (Fig 4), the spectra showed abnormalities when compared with the spectra of an age-matched subject (Fig 1). These abnormalities resemble similar changes in adrenoleukodystrophy (Fig 3) but do not include the presence of enhanced lipid resonances (indicative of active demyelination). Thus the proton MRS findings in the single Sanfilippo case are consistent with neuropathy; this may be due to excessive accumulation of mucopolysaccharides in neurons that can interfere with cell function resulting in neuronal death (2).

In Gaucher disease, accumulation of glucocerebrosides is due to an inherited deficiency in the enzyme glucocerebrosidase; this causes hepatosplenomegaly and bone lesions. Enzyme replacement, bone marrow transplantation, and, potentially, gene therapies constitute approaches to treatment (44). In the one 6-month-old child with Gaucher disease, MR findings were normal; proton MRS suggests encephalopathy with enhanced metabolites in the Glx and Inls area of the spectrum (Fig 5).

B and *C*, Localized proton MR spectra from the voxel indicated in *A*. *B*, Short-echo proton MR spectrum (2000/18) using STEAM. The elevated lipid resonances may indicate demyelination. In addition, increased peaks in the Glx/Inls areas of the spectrum indicate encephalopathy. *C*, Long-echo proton MR spectrum using PRESS (2000/270). No apparent accumulated lactic acid is detected. The relative heights of other metabolites are normal for age.

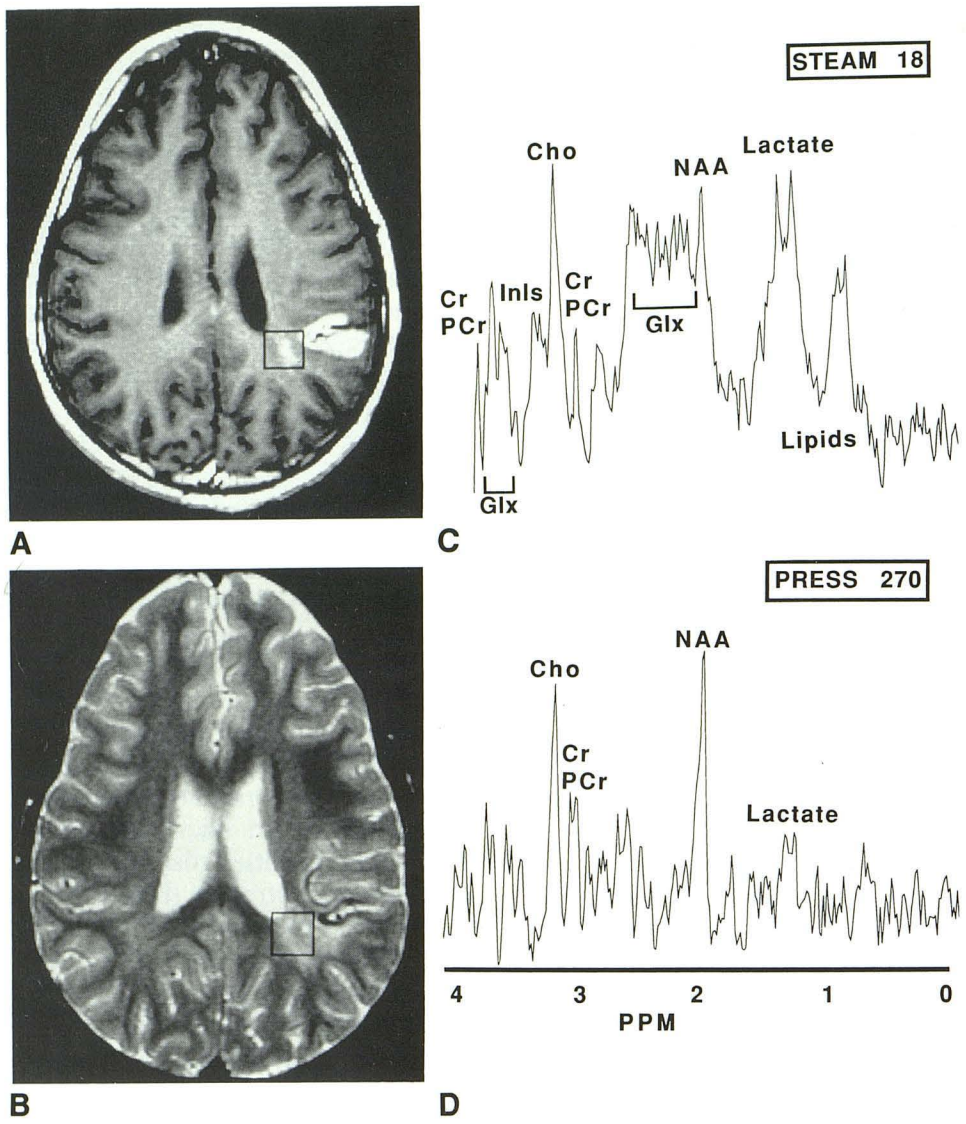

Fig. 9. Image-guided single-voxel proton MRS using a 2.2-cc voxel (*squares*) of interest chosen from axial brain MR images of a 9-year-old boy with subacute stroke.

A, T1-weighted image (500/12) after intravenous gadopentetate dimeglumine injection. Note enhancement of a compromised blood-brain barrier.

B, T2-weighted image (2500/100) shows hyperintensity in the periventricular white matter adjacent to the area of the stroke.

C and *D*, Localized proton MR spectra from the voxels indicated in *A* and *B*. *C*, Short-echo proton MR spectrum using STEAM (2000/18). Reduced NAA-to-Cho indicates neuronal degeneration. Increased peaks in the Glx/Inls areas of the spectrum indicate encephalopathy. Enhanced lipid peaks indicate demyelination; lactate is also detected. *D*, Long-echo proton MR spectrum using PRESS (2000/270). Minor accumulation of lactic acid was observed presumably because of the local perfusion deficit detected by dynamic contrast-enhanced perfusion MR imaging.

Hurler syndrome is associated with neonatal retardation. Reports of abnormal findings on imaging are limited (45). Electron microscopic studies show lysosomal accumulation of gangliosides. Mucopolysaccharide deficiency in a-i-iduronidase results in defective ganglioside metabolism and lipid accumulation within neurons (46). Neurodegeneration leads to brain atrophy manifested on MR. In the one child with Hurler syndrome, proton MRS findings indicated neurodegeneration by the low presence of NAA relative to Cho and increased presence of metabolites in the Glx and Inls areas of the spectrum.

Mitochondrial Dysfunction. Mitochondrial dysfunction results in cytopathies classified on a biochemical basis. Symmetrical or asymmetrical central-nervous-system defects, as well as defects in other organs such as muscle, liver, the hemo-

poietic system, and endocrine glands, can be caused by one or multiple enzyme deficiencies. Morphologic changes on computed tomography and MR do not indicate the specific enzymatic defect (42). Impaired aerobic metabolism of pyruvate results in anaerobic conversion to lactate and transamination to alanine (47). These substances can be detected in the serum. However, isolated increase of these substances may occur in the brain without their concomitant increase in serum. MRS may contribute to their detection by revealing located acidosis in the brain (48,49). In addition, demyelination occurs in Leigh disease (50).

In our proton MRS findings from a 4-month-old patient with Leigh disease, an excessive accumulation of lactate was detected in the voxel of interest placed in the lentiform nucleus. Others have shown lactate accumulation in image-guided proton MRS in the brains of patients with Leigh disease (48, 49). Our finding, however, was more pronounced and can be attributed either to a better location method or to site- and/or case-specific increased lactate accumulation.

Disorders in Amino Acid and Organic Acid Metabolism. The single case of an infant, with phosphorylase kinase deficiency, is representative of cases in which high levels of blood lactic acid are not accompanied by localized acidosis in brain. Proton MRS has been shown to be sensitive to changes of hepatic encephalopathy (16). The lack of such findings on proton MRS in this case may denote that hepatic dysfunction (consistent with high blood lactic acid levels) has not yet affected the brain.

Acquired Neurodegenerative Disorders

Hypoxic-Ischemic. The potential of MRS for studying brain metabolism in hypoxia or ischemia has been demonstrated by animal studies; energy-storing phosphate compounds (adenosine triphosphate and PCr) and tissue pH decrease, whereas intracellular phosphate and lactate increase (21, 51, 52). However, phosphorous MRS indicates that phosphorous-containing metabolite ratios are not sensitive indicators of functional impairment in chronic brain infarction (53). The change in total phosphate concentration observed reflects irreversible brain damage of the infarcted tissue. Whether an increase in lactate could be detected before an irreversible brain damage remains as a hypothesis that bears further examination. Proton MR spectra have been reported in subjects with stroke using long-echo (53, 54) and recently short-echo (18) localized MRS methods. In these studies, regions of infarction are associated with NAA depletion and marked increase in lactic acid, consistent with anaerobic glycolysis. However, heterogeneity within the lesion has not been addressed adequately because of the large voxels used. Our findings are in agreement with these previously reported studies. Use of a smaller voxel size may contribute additional information with regard to lesion heterogeneity by excluding surrounding brain edema from the involved area of infarction (Fig 9). The metabolite profiles are not altered by a possible diluting effect of the edema, thus allowing better assessment of white matter adjacent to the stroke. The reduction in NAA rather than its absence is indicative of the NAA pool stability and suggests an active degradation in injured neurons during the first days of an infarct. It has been hypothesized that aminohydrolase, a membrane-bound enzyme in healthy neurons, may be released in neuronal injury (18). The reduction in creatines (Cr and PCr) observed by us (Fig 9) and others (18) could be caused by a reduction in total Cr by either a catabolic (PCr being catabolized to Cr) and/or extracellular leakage process. Cho-containing compounds are normally resistant to ischemic degradation and thus did not appear to decrease. An additional finding using short-echo-stimulated echoes is the enhanced Glx and Inls peaks in addition to reduced NAA. This finding may indicate neurotransmitter imbalance and/or neurodegeneration and is supported by analytic findings of reduced NAA in neurons associated with excitatory neurotransmitter-induced lesions in the rat brain (55). Accumulation of excitatory amino-acid neurotransmitters, secondary to hypoxia-ischemia (56), has been implicated in the induction of neuronal death (57). Thus if reduction in NAA and elevation in Glx and Inls constitute early signs of neurodegeneration, then proton MRS could detect neurodegeneration before an irreversible stage.

Toxic Encephalopathies. Animal data suggest that intrauterine or postnatal cocaine exposure during periods of rapid brain maturation may have permanent effects on behavior (58). The question remains whether intrauterine cocaine exposure leads to encephalopathy in childhood. Our limited experience of two cases cannot preclude the utility of proton MRS in assessing permanent alterations induced by such toxic effects.

The proton MRS findings in all our cases of neurodegenerative diseases of childhood can be summarized and interpreted as follows: 1) reduction of NAA-to-Cho ratio (neuronal loss and gliosis); 2) increased mobile lipid peaks (demyelination); 3) enhanced Glx and Inls (neurotrans-

mitter neurotoxicity hypothesis); and 4) detection of lactic acid (metabolic acidosis).

These findings by proton MRS are not limited to a particular central-nervous-system disorder. Rather, they are indicative of metabolic disturbances associated with encephalopathy (either static or progressive) and thus contribute to MR assessment of neurodegenerative disorders. Their value may lie in following disease progression and assessing therapeutic intervention, because both of these processes may affect metabolism of involved tissue and organs. In addition, the prognostic value and importance in early detection of these conditions require further investigation. Assessment of neurodegenerative changes may require an understanding of regulatory mechanisms involving excitatory-amino-acid cytotoxicity. These have been implicated in an increasing number of neurodegenerative conditions (39, 59–62). The hypothesis is based on experimental evidence that excitatory-amino-acid neurotoxicity (dependent on calcium concentration) is mediated by excitatory-amino-acid receptors (63–65). These receptors permit influx of calcium into cells, thus inducing phosphatidyl-Inls turnover and liberating Inls phosphates (40, 41). This results in translocation and activation of protein kinase C (66), ultimately causing the destruction of these cells. It may thus be plausible that the Glx and Inls metabolites detected by short-echo proton MRS in vivo in the present study indicate excitatory-amino-acid toxicity. Excitatory-amino-acid toxicity changes may be reversed by appropriate pharmacologic intervention; this would prevent irreversible structural and neuropathologic deterioration.

Conclusions

Proton MRS shows changes of metabolites in neurodegenerative disorders. In hereditary neurodegenerative disorders, the observed changes can be attributed to metabolic defects. In acquired neurodegenerative cases, such as hypoxia-ischemia and toxic encephalopathy, proton MRS findings are related to metabolic disturbances caused by endogenous or exogenous factors affecting cellular metabolism. In addition, neurochemical imbalances associated with the degenerative process may be detected; this contributes to our in vivo understanding of neurodegenerative disorders. These MRS findings may assist and be complimentary to MR in both diagnostic assessment and monitoring of therapy of neurodegenerative disorders.

Acknowledgments

We thank Sarah Nelson, PhD, for review of the manuscript. We also thank the Signa Spectroscopy group of General Electric Medical Systems, especially Peter Webb, PhD, Ralph Hurd, PhD, Tom Raidy, PhD, and Yuri Wedmid, PhD, for their support and encouragement. We appreciate the administrative assistance of Ms. Brenda Moore. Thanks to Dr. Derek C. Harwood-Nash for useful discussions.

References

1. Valk J, Van der Knaap MS. Classification of myelin disorders. In: Becker LE, Yates A, eds. *Magnetic resonance of myelin, myelination and myelin disorders.* Berlin: Springer-Verlag, 1989:4–8
2. Becker LE, Yates A. Inherited metabolic disease. In: Valk J, Van der Knaap MS, eds. *Textbook of neuropathology.* Baltimore: Williams & Wilkins, 1990:331–427
3. Mirowitz SA, Sartor K, Prensky AJ, Gado M, Hodges FJI. Neurodegenerative diseases of childhood: MR and CT evaluation. *J Comput Assist Tomogr* 1991;15:210–222
4. Van der Knaap MS, Valk J, De Neeling N, Nauta JJP. Pattern recognition in magnetic resonance imaging of white matter disorders in children and young adults. *Neuroradiology* 1991;33:478–493
5. Barkovich AJ, Kjos BO, Jackson DEJ, Norman D. Normal maturation of the neonatal and infant brain: MR imaging at 1.5 T. *Radiology* 1988;166:173–180
6. Arnold DL, Matthews PM, Francis G, Antel J. Proton magnetic resonance spectroscopy of human brain in vivo in the evaluation of multiple sclerosis: Assessment of the load of disease. *Magn Reson Med* 1990;14:154–159
7. Van Hecke P, Marchal G, Johannik K, et al. Human brain proton localized NMR spectroscopy in multiple sclerosis. *Magn Reson Med* 1991;18:199–206
8. Grodd W, Krägeloh-Mann I, Klose U, Sauter R. Metabolic and destructive brain disorders in children: findings with localized proton MR spectroscopy. *Radiology* 1991;181:173–181
9. Frahm J, Bruhn H, Gyngell ML, Merboldt KD, Hanicke W, Sauter R. Localized high-resolution proton NMR spectroscopy using stimulated echoes: initial applications to human brain in vivo. *Magn Reson Med* 1989;9:79–93
10. Michaelis T, Merboldt KD, Hänicke W, Gyngell ML, Bruhn H, Frahm J. On the identification of cerebral metabolites in localized ^{1}H spectra of human brain in vivo. *NMR Biomed* 1991;4:90–98
11. Frahm J, Merboldt KD, Hänicke W. Localized proton spectroscopy using stimulated echoes. *J Magn Reson* 1987;72:502–508
12. Bottomley PA. Spatial localization in NMR spectroscopy in vivo. *Ann NY Acad Sci* 1987;508:333–348
13. Pauly J, Le Roux P, Nishimura D, Macovski A. Parameter relations for Shinnar-Le Roux selective excitation pulse design algorithm. *IEEE Trans Biomed Imag* 1991;10:53–65
14. Moonen CTW, Von Kienlin M, Van Ziil PCM, et al. Comparison of single-shot localization methods (STEAM and PRESS) for in vivo proton NMR spectroscopy. *NMR Biomed* 1989;2:201–208
15. Rothman DL, Hanstock CC, Petroff AC, Novotny EJ, Prichard JW, Shulman RG. Localized ^{1}H NMR spectra of glutamate in the human brain. *Magn Reson Med* 1992;25:94–106
16. Kreis R, Ross BD, Farrow NA, Ackerman Z. Metabolic disorders of the brain in chronic hepatic encephalopathy detected with H-1 MR spectroscopy. *Radiology* 1992;182:19–27
17. Hahn EL. Spin echoes. *Physiol Rev* 1950;80:580–594
18. Bruhn H, Frahm J, Gyngell ML, Merboldt KD, Hanicke W, Sauter R. Cerebral metabolism in man after acute stroke: new observations using localized proton NMR spectroscopy. *Magn Reson Med* 1989;9:126–131
19. Ernst T, Henning J. Coupling effects in volume selective ^{1}H spectroscopy of major brain metabolites. *Magn Reson Med* 1991;21:82–96
20. Haase A, Frahm J, Haenicke W, Matthei D. ^{1}H NMR chemical shift selective (CHESS) imaging. *Phys Med Biol* 1985;30:341–344
21. Behar KL, Den Hollander JA, Stromski ME, Ogino T, Shulman RG. High-resolution ^{1}H nuclear magnetic resonance study of cerebral hypoxia in vivo. *Proc Natl Acad Sci USA* 1983;80:4945–4948

22. Behar KL, Ogino T. Assignment of resonances in the ^{1}H spectrum of rat brain by two-dimensional shift correlated and J-resolved NMR spectroscopy. *Magn Reson Med* 1991;17:285–303
23. Kauppinen RA, Kokko H, Williams SR. Detection of mobile proteins by proton nuclear magnetic resonance spectroscopy in the guinea pig brain ex vivo and their partial purification. *J Neurochem* 1992;58:967–974
24. Kauppinen RA, Palvimo J. Contribution of cytoplasmic polypeptides to the ^{1}H NMR spectrum of developing rat cerebral cortex. *Magn Reson Med* 1992;25:398–407
25. Peden CJ, Cowan FM, Bryant DJ, et al. Proton MR spectroscopy of the brain in infants. *J Comput Assist Tomogr* 1990;14:886–894
26. Burri R, Bigler P, Straehl P, Posse S, Colombo JP, Herschkowitz N. Brain development: ^{1}H magnetic resonance spectroscopy of rat brain extracts compared with chromatographic methods. *Neurochem Res* 1990;15:1009–1016
27. Bates TE, Williams SR, Gadian DG, Bell JD, Small RK, Iles RA. ^{1}H NMR study of cerebral development in the rat. *NMR Biomed* 1989;2:225–229
28. Van der Knaap MS, Van der Grond J, Van Rijen PC, Faber JA, Valk J, Willemse K. Age-dependent changes in localized proton and phosphorus MR spectroscopy of the brain. *Radiology* 1990;176:509–515
29. Miller G, Ramer JC. *Static encephalopathies of infancy and childhood.* New York: Raven, 1992
30. Moser HW. Peroxisomal disorders. *Clin Biochem* 1991;24:343–351
31. Moser HW, Bergin A, Cornblath D. Peroxisomal disorders. *Biochem Cell Biol* 1991;69:463–474
32. Van der Knaap MS, Valk J. The MR spectrum of peroxisomal disorders. *Neuroradiology* 1991;33:30–37
33. Kumar AJ, Rosenbaum AE, Naidu S, et al. Adrenoleukodystrophy: correlating MR imaging with CT. *Radiology* 1987;165:497–504
34. Lazo O, Contreras M, Hashmi M, Stanley W, Irazu C, Singh I. Peroxisomal lignoceroyl-CoA ligase deficiency in childhood adrenoleukodystrophy and adrenomyeloneuropathy. *Proc Natl Acad Sci USA* 1988;85:7647–7651
35. Brown FR III, Chen WW, Kirschner DA, et al. Myelin membrane from adrenoleukodystrophy brain white matter: biochemical properties. *J Neurochem* 1983;41:341–348
36. Moser HW, Moser AE, Singh I, O'Neill BP. Adrenoleukodystrophy: survey of 303 cases: biochemistry, diagnosis, and therapy. *Ann Neurol* 1984;16:628–641
37. Nadler JV, Cooper JR. N-acetyl-L-aspartic acid content of human neural tumours and bovine peripheral nervous tissues. *J Neurochem* 1972;19:313–319
38. Tallan HH. Studies on the distribution of N-acetyl-L-aspartic acid in brain. *J Biol Chem* 1957;224:41–45
39. McDonald JW, Johnson MV. Physiological and pathophysiological roles of excitatory amino acids during central nervous system development. *Brain Res Rev* 1990;15:41–70
40. Sladeczek F, Pin JP, Recasens M, Bockaert J, Weiss S. Glutamate stimulates inositol phosphate formation in striatal neurons. *Nature* 1986;317:717–719
41. Nicoleti F, Meek JL, Iadarola MJ, Chuang DM, Roth BL, Costa E. Coupling of inositol phospholipid metabolism with excitatory amino acid recognition sites in rat hippocampus. *J Neurochem* 1986;46:40–46
42. Becker LE. Lysosomes, peroxisomes and mitochondria: function and disorder. *AJNR: Am J Neuroradiol* 1992;13:609–620
43. Kendal BE. Disorders of lysosomes, peroxisomes and mitochondria. *AJNR: Am J Neuroradiol* 1992;13:621–653
44. Beutler E. Gaucher disease: new molecular approaches to diagnosis and treatment. *Science* 1992;256:794–799
45. Afifi AK. Computed tomography and magnetic resonance imaging of the brain in Hurler's disease. *J Child Neurol* 1990;5:235–241
46. Susuki K. Ganglioside patterns of normal and pathological brain. In: Aronson SM, Volk BW, eds. *Inborn disorders of sphengolipid metabolism.* Oxford: Pergamon, 1967:215–226
47. Erven PMM, Ruitenbeek FJM, Renier WO. Disturbed oxidative metabolism in subacute necrotizing encephalopathy (Leigh syndrome). *Neuropediatrics* 1986;17:28–32
48. Krageloh-Mann I, Grodd W, Nieman G, Haas G, Ruitenbeek W. Assessment and therapy monitoring of Leigh Disease by MRI and proton spectroscopy. *Pediatr Neurol* 1992;8:60–64
49. Detre JA, Wang Z, Bogdan AR, et al. Regional variation in brain lactate in Leigh syndrome by localized ^{1}H magnetic resonance spectroscopy. *Ann Neurol* 1991;29:218–221
50. Kimura S, Kobayashi T, Amemiya. Myelin splitting in the spongy lesion in Leigh encephalopathy. *Pediatr Neurol* 1991;7:56–58
51. Gadian DG, Frackowiak RS, Crockard HA, et al. Acute cerebral ischemia: concurrent changes in cerebral blood flow, energy metabolism, pH, and lactate measured with hydrogen clearance and ^{31}P and ^{1}H nuclear magnetic resonance spectroscopy. I. Methodology. *J Cereb Blood Flow Metab* 1987;7:199–206
52. Crockard HA, Gadian DG, Frackowiak RS, et al. Acute cerebral ischemia: concurrent changes in cerebral blood flow, energy metabolism, pH and lactate measured with hydrogen clearance and ^{31}P and ^{1}H nuclear magnetic resonance spectroscopy. II. Changes during ischaemia. *J Cereb Blood Flow Metab* 1987;7:394–402
53. Bottomley PA, Drayer BP, Smith LS. Chronic adult cerebral infarction studied by phosphorus NMR spectroscopy. *Radiology* 1986;160:763–766
54. Berkelbach van der Sprenkel JW, Luyten PR, van Rijen PC, Tulleken CAF, den Hollander JA. Cerebral lactate detected by regional proton magnetic resonance spectroscopy in a patient with cerebral infarction. *Stroke* 1988;19:1556–1560
55. Koller KJ, Zaczek R, Coyle JT. N-Acetyl-aspartyl-glutamate: regional levels in rat brain and the effects of brain lesions as determined by a new HPLC method. *J Neurochem* 1984;43:1136–1142
56. Hagberg H, Lehman A, Sandberg M, Nystrom B, Jacobson I, Hamberger A. Ischemia-induced shift of inhibitory and excitatory amino acids from intra- to extracellular compartments. *J Cereb Blood Flow Metab* 1985;5:413–419
57. Rothman SM. Synaptic release of excitatory amino acid neurotransmitter mediates anoxic neuronal death. *J Neurosci* 1984;4:1884–1891
58. Wasiewski WW. Central nervous system effects of cocaine in children. In: Miller G, Ramer JC, eds. *Static encephalopathies of infancy and childhood.* New York: Raven, 1992:325–330
59. Beal MF, Kowall NW, Ellison DW, Masurek MF, Swartz KJ, Martin JB. Replication of the neurochemical characteristics of Huntington's disease by quinolinic acid. *Nature* 1986;321:168–171
60. Dure LS, Young AB, Penney JB. Excitatory amino acid binding sites in the caudate nucleus and frontal cortex of Huntington's disease. *Ann Neurol* 1991;30:785–793
61. Young AB, Greenamyre JT, Hollingsworth Z, et al. NMDA receptor losses in putamen from patients with Huntington's disease. *Science* 1988;241:981–983
62. Choi DW. Glutamate neurotoxicity and diseases of the nervous system. *Neuron* 1988;1:623–634
63. Mayer ML, Westbrook GL. The physiology of excitatory amono acids in the vertebrate central nervous system. *Prog Neurobiol* 1987;28:197–276
64. Choi DW. Ionic dependence of glutamate neurotoxicity. *J Neurosci* 1987;7:369–379
65. Murphy SN, Thayer SA, Miller RJ. The effects of excitatory amino acids on intracellular calcium in single mouse striatal neurons in vitro. *J Neurosci* 1987;7:4145–4158
66. Nishimura Y. Studies and perspectives of protein kinase C. *Science* 1986;233:305–312

Please see the Commentary by Zimmerman on page 1282 in this issue.